NANO LETTERS

Letter

Two-Terminal Nanoelectromechanical Devices Based on Germanium Nanowires

Jana Andzane, Nikolay Petkov, Aleksandrs I. Livshits, John J. Boland, Justin D. Holmes, and Donats Erts

Nano Lett., **2009**, 9 (5), 1824-1829• Publication Date (Web): 26 March 2009

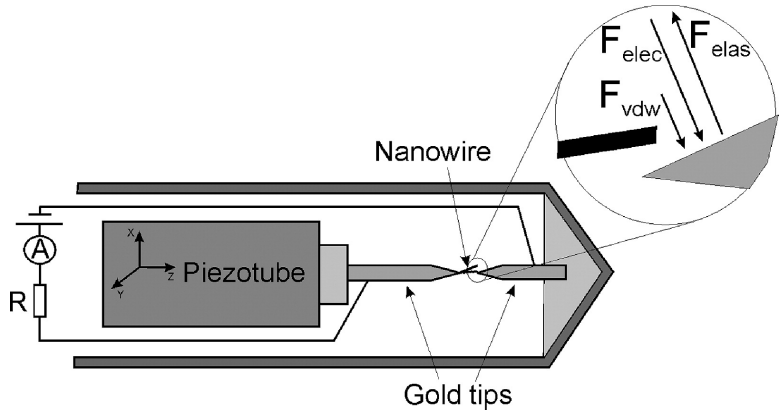

More About This Article

Additional resources and features associated with this article are available within the HTML version:

- Supporting Information
- Access to high resolution figures
- Links to articles and content related to this article
- Copyright permission to reproduce figures and/or text from this article

View the Full Text HTML

NANO LETTERS

2009
Vol. 9, No. 5
1824-1829

Two-Terminal Nanoelectromechanical Devices Based on Germanium Nanowires

Jana Andzane,[‡] Nikolay Petkov,[§,†] Aleksandrs I. Livshits,[‡] John J. Boland,[ϕ] Justin D. Holmes,[*,†,ϕ] and Donats Erts[*,‡,ϕ]

Institute of Chemical Physics, University of Latvia, Riga, Latvia, Materials and Supercritical Fluids Group, Department of Chemistry and the Tyndall National Institute, University College Cork, Cork, Ireland, Electron Microscopy and Analysis Facility, Tyndall National Institute, Lee Maltings, Prospect Row, Cork Ireland, and Centre for Research on Adaptive Nanostructures and Nanodevices (CRANN), Trinity College Dublin, Dublin 2, Ireland

Received December 15, 2008; Revised Manuscript Received March 2, 2009

ABSTRACT

A two-terminal bistable device, having both ON and OFF regimes, has been demonstrated with Ge nanowires using an *in situ* TEM−STM technique. The function of the device is based on delicately balancing electrostatic, elastic, and adhesion forces between the nanowires and the contacts, which can be controlled by the applied voltage. The operation and failure conditions of the bistable device were investigated, i.e. the influence of nanowire diameter, the surface oxide layer on the nanowires and the current density. During ON/OFF cycles the Ge nanowires were observed to be more stable than carbon nanotubes, working at similar conditions, due to the higher mechanical stability of the nanowires. The higher resistivity of Ge nanowires, compared to carbon nanotubes, provides potential application of these 1D nanostructures in high-voltage devices.

Nanoelectromechanical systems (NEMS) have recently attracted much attention due to their unique properties and possible applications, that differ greatly from those of existing microelectromechanical systems (MEMS).[1] Typical examples of NEMS are ultrahigh-frequency resonators,[1−8] nanotweezers,[9,10] nanorelays and switches,[11−19] memory and logic elements,[13,16,20] and sensors for dispalacement, force, mass, and charge detection.[2,21−23,29] In NEMS the critical dimensions of the moving elements is on the nanometer scale, and therefore the displacement of these elements is extremely small. As a result the internal operating frequencies of NEMS may achieve giga- and terahertz frequencies.[4,23] Significantly, the power consumption and heat capacity of a NEM device can be extremely low. Moreover, in NEMS the device density can reach much higher levels compared to that in MEM devices, e.g. densities of 10^{11} cm^{-2} have been shown for crossed nanowire resonators.[30]

The basic operating principle underlying ON/OFF NEMS (switches, nanorelays, nanotweezers) is the strong electromechanical coupling between the nanobeam and the electrodes, whereas the electrostatic and elastic forces associated with device operation are comparable with the adhesive forces that hold these devices together.[31] During the past few years, carbon nanotubes have emerged as promising components in NEM devices.[1,5,9−12,15,18,20,31] However, other materials such as metals,[6,7] silicon nitride,[3,21] TiN,[17] semiconductor nanowire,[2,13,32] and DNA molecules[14] have also been integrated as active elements in NEMS. Single crystalline nanowires are excellent candidates for NEM devices due to their uniform chemical and physical structure, low mass, and good structural and compositional reproducibility. Additionally, nanowires can be fabricated as ordered arrays[33] with densities of up to 2×10^{12} cm^{-2}.

While most ON/OFF NEMS operate as three-terminal devices,[11,12,15,17,19] two-terminal ON/OFF NEM devices have been investigated both theoretically[34,35] and experimentally.[10,13,15,17−19,32,36] Experimentally, the operation of two-terminal ON/OFF devices has been demonstrated using carbon nanotubes[10,15,18,36] and lithographically fabricated TiN cantilevers[17] as active elements. The operation of Si and Ge nanowires in two-terminal NEMS has also been demonstrated;[13,32] however, the operation of Ge nanowires was demonstrated only in an ON regime.[13] A systematic investigation of the operation of two-terminal NEMS having

* Corresponding authors. E-mail: j.holmes@ucc.ie and donats.erts@lu.lv.
‡ Institute of Chemical Physics, University of Latvia, Riga, Latvia.
† Materials and Supercritical Fluids Group, Department of Chemistry and the Tyndall National Institute, University College Cork.
§ Electron Microscopy and Analysis Facility, Tyndall National Institute.
ϕ Centre for Research on Adaptive Nanostructures and Nanodevices (CRANN), Trinity College Dublin.

10.1021/nl8037807 CCC: $40.75
Published on Web 03/26/2009

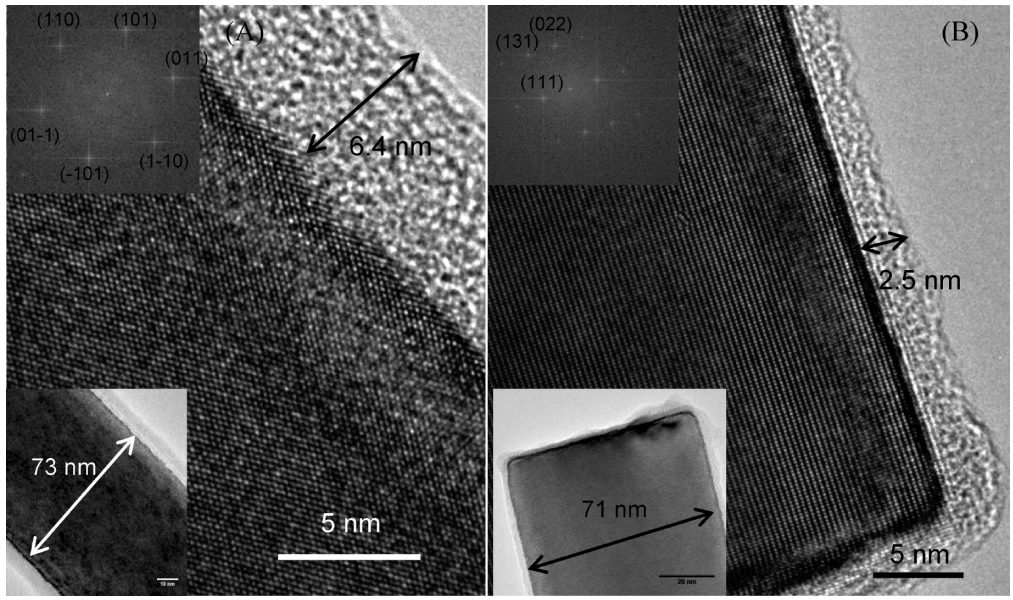

Figure 1. HRTEM images of two different Ge nanowires both grown along the [110] direction with similar diameters but having a different surface oxide thickness: (A) a Ge nanowire viewed along the [111] zone axis with a 6.4 nm oxide layer on the {211} set of planes terminating at the nanowire surface and (B) a Ge nanowire viewed along the [211] zone axis with a 2.5 nm oxide layer on the {111} set of planes terminating at the nanowire surface.

semiconductor nanowires as basic functioning units has not yet been demonstrated.

In this paper we present an *in situ* investigation of the operational conditions of a mechanically stable two-terminal ON/OFF NEM device based on Ge nanowires. The advantage of using *in situ* techniques is that the switching process can be visualized during the experiments. Additionally, the position of the contacts and the length of the nanobeam, from the clamping point to the contact with the opposite electrode, can be adjusted within the system without the need to prepare new specimens. This level of flexibility cannot be achieved when NEM devices are prepared by electron beam lithography and other techniques.

The Ge nanowires were grown from gold nanoparticles using a supercritical fluid method as described previously.[37] The nanowires were clamped to the gold tip with conductive epoxy, providing a large contact area to the electrode in comparison to the contact at the free end of the nanowire which was established during a switching event. The Ge nanowires synthesized were single crystalline in nature, with varying diameters, ranging from 10−150 nm, and lengths ranging from 1−25 μm. Figure 1 shows HRTEM images of the Ge nanowires synthesized, depicting their single crystalline nature and the existence of an amorphous GeO_x layer on their surface. Fast Fourier transforms (FFT) of the HRTEM were used to determine their growth direction. For example, the Ge nanowire shown in Figure 1A, has a diameter of 73 nm, a mean oxide shell thickness of 6.4 nm and a [110] growth direction. A Ge nanowire with a similar diameter, grown along the same growth direction but with a much thinner oxide layer, is shown in Figure 1B. Statistical analysis of a large population of nanowires showed that the primary growth direction of the nanowires was along the [110] direction, with other possible growth directions being [111], [211], and [311]. The thickness of the amorphous Ge oxide was found to vary, depending on the type of planes terminating the nanowire surface and the time the nanowires were exposed to ambient atmosphere (see examples in Figure 2). For nanowires kept at ambient conditions for 4 weeks, the average oxide thickness was found to be around 4 nm, with the highest and lowest thickness observed on {211} and {110} surface planes, respectively.

The operation conditions of a NEM device using Ge nanowires, but functioning only in the ON regime, has already been reported.[13] This Ge nanowire device operated at voltages below 10 V and at a very small distance between the nanowire tip and the opposite electrode. When designing two-terminal ON/OFF devices, one should take into consideration that the initial distance between the end of the nanowire and the electrode should be large enough to avoid spontaneous jump-to-contact movement caused by van der Waals attractive forces. Performing ON/OFF operations with the device is then possible by assuring that the sum of the electrostatic and van der Waals forces acting between the nanowire tip and the opposite electrode is high enough to overcome the elastic force of the nanowire (ON operation), and subsequently that the elastic force exceeds the total attractive force (adhesion and electrostatic) at the contact during an OFF operation. As a consequence, the operation voltages for ON/OFF devices must be higher than those operating only in an ON regime. The effects caused by high current densities also have to be taken into account. In spite of the high resistivity of Ge (0.5 Ω.m[38]), for small contact areas around 100 nm^2, the operational current densities may be higher than 10 nA nm^{-2} which is the current density limit for nanometer-sized metallic wires.[39] In order to decrease the current through the contact in some NEM devices, the surface of one of the electrodes can be coated with an insulating layer[10,17,36] or a resistor can be added in series.[18]

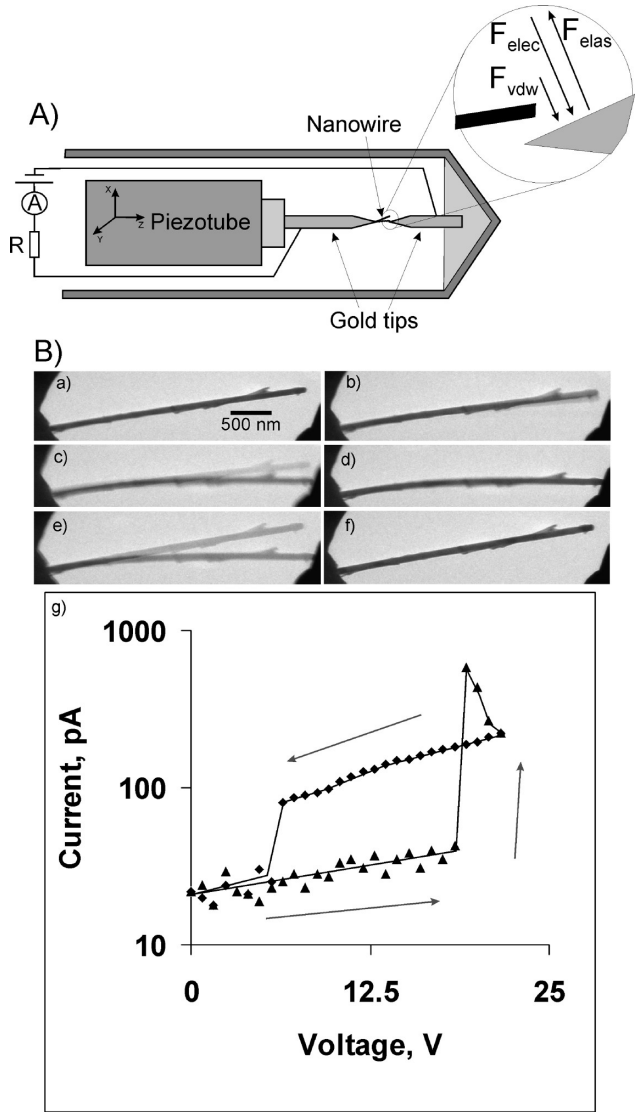

Figure 2. (A) TEM−SPM experimental setup for the *in situ* investigation of a nanowire-based NEM device and (B) TEM image sequence and corresponding $I-V$ curve showing the behavior of the Ge nanowire during a voltage sweep: (a) the initial position of the nanowire and the electrode, (b) after a voltage increase, (c) a jump-to contact event over a distance of 250 nm at 19 V, (d) the nanowire in contact with the counter electrode, (e) the nanowire jumps-off-contact when the voltage is decreased to 6 V, (f) the nanowire returns to the initial position when voltage decreases to 0. and (g) shows the $I(V)$ profile.

A schematic of our nanowire-based two-terminal NEM device is shown in Figure 2(a). The forces acting between the nanowire and the opposite electrode in a two-terminal NEM device are shown as an inset in Figure 2. A scanning tunneling microscope compatible with a transmission electron microscope (TEM−STM)[40,41] was employed in our experiments to characterize our device. Figure 2b shows a TEM image sequence illustrating the behavior of a Ge nanowire, with a length of 3 μm and a radius of 30 nm, during a voltage sweep between 0 and 23 V. The initial distance between the end of the nanowire and the opposite electrode was approximately 500 nm. When a voltage between the electrodes is applied, the nanowire deforms and moves toward the opposite electrode (Figure 2b). At a voltage of 19 V the nanowire end was approximately 250 nm from the surface of the opposite electrode. At this position, the gradient of the attractive tip−sample force exceeds the spring constant of the nanowire and jump-to-contact occurs (panels c and d of Figure 2). Simultaneously, on the $I-V$ curve at 19 V a sharp increase of the current, from a noise level of between 30 and 50 pA up to 0.8 nA, was observed (Figure 2g). The nanowire stayed in contact with the counter electrode during a further voltage increase up to 23 V and subsequent backward decrease down to 6 V. At 6 V the attractive force acting between the nanowire and the electrode was lower than the elastic force of the bent nanowire and at that moment a jump-off-contact was observed (Figure 2e). Subsequently a fast current drop was detected in the $I(V)$ characteristic during this switching-off event. The $I(V)$ curve exhibited a hysteresis loop[12,18] which was induced by the adhesion forces in the contact.

In theory, the operation of the two-terminal ON/OFF NEM device can be varied by changing (i) the elastic force of the nanowire, e.g. by changing the diameter and the length of the nanowire as well as the thickness of the surface oxide layer, or (ii) the adhesion forces at the contact by using different contact materials. Experimentally we find that the initial operation distance between the electrode and the nanowire has to be increased when the radii of the nanowires is increased. Table 1 shows that the jump-off-contact distance increases from 250 nm up to 5 and 10 μm when nanowires with radii of 30, 75, and 150 nm, respectively, were used (see Figures 2, 3 and Figure S1 in Supporting Information for relevant TEM image sequences). We estimate that the adhesion forces, (446 and 456 nN for nanowires with radii of 75 and 150 nm, respectively) and elastic forces (450 and 475 nN for nanowires with radii of 75 and 150 nm, respectively) are almost equal for both NEM devices (see Table 1). On the contrary the calculated adhesion force for a Ge nanowire with a radius of 30 nm was 167 nN, thus being an order of magnitude higher than the elastic force of the nanowire which was calculated to be 15 nN. We attribute the difference between the adhesive and elastic forces for a 30 nm diameter nanowire due to the variation in the thickness of the oxide layer on different facets of the nanowires (see, for example, Figure 1), leading to an uneven contact and hence a lower contact area than expected.

Additionally, the presence of a native oxide layer implies some limitations on device operation at low voltages. $I(V)$ characteristic from a Ge nanowire device, Figure 3h, show that a nonconductive gap is observed for nanowires coated with a native oxide layer. For different wires the nonconductive gap varied between 1 and 6 V. The resistivity of these nanowires measured in a two-contact configuration exceeded the resistivity of bulk Ge, from several times up to 2 orders of magnitude. We attribute this range due to variations in the thickness of the oxide layer on different surface facets of the nanowires, as seen by transmission electron microscopy (Figure 1). For NEMS operation below 2−4 V, the oxide layer needs to be removed from the nanowire surface in order to obtain a functioning device. The ON/OFF operation of such a NEM device, in which

Table 1. Dimensions and Operating Conditions of Ge Nanowires in NEM Devices as Shown in the Corresponding Figures

	Figure 2	Figure S1	Figure 3	Figure S2	Figure 4 a−d	Figure 4 e−g
radius, nm	30	150	75	50	60 175[a]	80
length, μ	3	25	7	6.5	4.5	17
electrode radius, nm	100	115	420	1300	600	2100
jump-to-contact distance, nm	250	10 000	5 000	500	1000	600
jump-to-contact voltage, V	19	28	35	13.5	31	37
jump-off-contact voltage, V	6	1.2	0	0	16	–
contact area, nm^2	78	331	321	259	218 1030[a]	418
adhesion force, nN	165	456	446	383	339 1030[a]	538
elastic force, nN	14.5	475	450	177	140	10
max current, nA	0.6	50	10	1050	140	1.5[a]
current density[a] in nanowire, A/m^2 $\times$ 10^{-6}	0.21	0.71	0.57	134	12.4	0.075[b]
current density[a] in contact, A/m^2 $\times$ 10^{-6}	6.3	125	22	10 000	424	6.7[b]

[a] After ball formation/after melting. [b] Real current was not measured.

the oxide layer was removed by ion etching just before measurement, is shown in panels a−g of Figure 3. Indeed, the $I(V)$ characteristics of this device showed linear ohmic behavior after oxide removal (Figure 3h). The nanowire, with a radius of 75 nm and length of 7 μm, jumped into contact with the electrode surface from a distance of 5 μm at a voltage of 35 V and jumped off contact at a voltage of 0 V (Figure 3a−f). The current could be easily measured down to 0 V (Figure 3g) even when an additional resistance of 100 MΩ was used in series for controlling the current. The resistivity of the nanowire with the removed oxide layer measured in two-contact configuration was 0.5 Ω m and corresponds to the resistivity of bulk Ge.

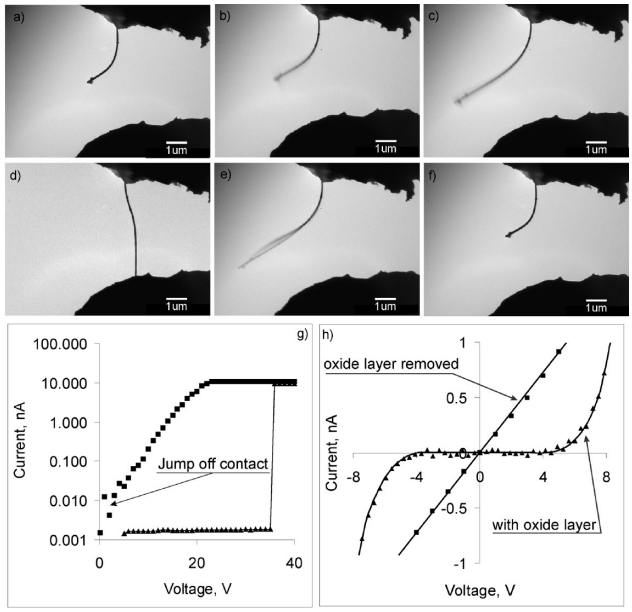

Figure 3. TEM images of the Ar-ion-treated Ge nanowire: (a) the initial position of the nanowire and electrodes, (b) and (c) the nanowire's motion toward the counter electrode during a voltage sweep between the electrodes, (d) the nanowire is in contact with the counter electrode (jump-to-contact occurred at 35 V), (e) and (f) the nanowire jumps-off-contact when the voltage reduces to 1.5 V and returns to the initial position, (g) corresponding $I(V)$ characteristics and (h) $I(V)$ characteristics of oxide-coated nanowires without and with Ar-ions treatment. I(V) characteristics were measured in contact.

The ON/OFF NEM devices that we investigated showed remarkable durability. Neither melting nor damage of the nanowires was observed after tens of repeated measurements. For comparison, bistable devices based on carbon nanotubes having similar dimensions, e.g. carbon nanotube lengths of 1−20 μm and diameters of 10−130 nm, with a distance between the nanotube end and the counter electrode of 0.5−2.0 μm, at a jump-to-contact voltage of 28 V and a 0.98 GΩ additional resistor in the circuit, shortened whenever jumping into contact with the electrode occurred.[18] A possible reason for the high durability of the nanowires is the defect-free, single crystalline nature of the Ge nanowire, resulting in their strength being close to the theoretical limit of 15 GPa,[42] which is an order of magnitude higher than that for carbon nanotubes.

To determine the operation limits of the Ge nanowire-based NEM devices the behavior of nanowires at higher current densities were investigated. Figure 4 shows the stability of the oxide-coated and oxide-free nanowires when current densities of 3−4 orders of magnitude higher than those used in previous experiments were allowed to flow through the devices (Table 1). Both modifications and damage at the end of the nanowires, as well as along the full length of the nanowire, were observed at high current densities. For example, a and d of Figure 4 show shortening of the nanowire followed by the formation of a ball, with the radius larger than the radius of the nanowire (175 and 60 nm, respectively). For these devices the maximum permitted current was set higher in comparison to that for previous devices, at 1 μA. The ball was formed immediately after jump-to-contact at 13.5 V, at a nanowire−electrode separation of 500 nm. Surprisingly the current changes during the increase and decrease of the voltage were monotonic without abrupt alternations (normally sharp and abrupt changes in the $I(V)$ characteristics are observed after nanowire shortening, (Figure S2 in Supporting Information). We believe that during the melting of the nanowire the electrical properties of the contact are improved, and as a result the

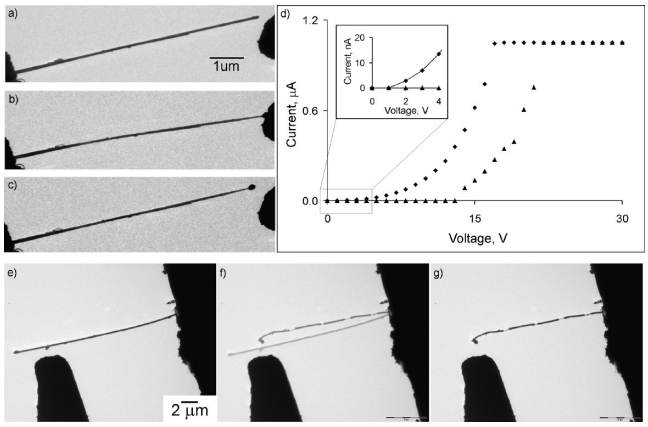

Figure 4. (a−d) Melting of the end of an Ar-ion-treated nanowire due to the high current through the contact: (a) the initial position and geometry of the nanowire, (b) jump-to-contact and immediate melting of the end of the nanowire at 13.5 V, (c) jump-off-contact with a few seconds delay after the voltage was switched off, (d) the corresponding $I(V)$ curve, (e) and (f) failure of the nanowire at the moment when direct contact between the nanowire and the electrode was achieved ((e) the nanowire in its initial position and (f) a moment before/after contact with the counter electrode at a voltage of 37 V), and (g) the core of the nanowire melts and divides into separate drops inside the outer germanium oxide tube.

nanowire exhibits a higher conductivity during the voltage decrease as compared to the voltage increase. Nevertheless, a detailed analysis of the microstructure of the nanowire-contact area is required for a further understanding of this process. When no current limitations were applied to some devices, complete melting of the nanowires was observed during the jump-to-contact event. Panels e and g of Figures 4 show melting of a nanowire when a jump-to-contact event occurred at 37 V from a distance of 500 nm. The nanowire (radius of 80 nm and length of 17 μm) melted in a very short time; hence, in one image (Figure 4f), the nanowire was captured 'in motion' before the jump-to-contact event and immediately after it. As observed, the core of the nanowire melted and divided into separate segments inside the outer germanium oxide shell, suggesting that the temperature of the nanowire was higher than the melting point of Ge (bulk is 938 °C) but did not exceed the melting temperature of GeO_x (1115 °C). We were unable to detect the current through the nanowires because the current pulse was shorter than the registration time of our system. The detected current was only 1.5 nA. Simulations were performed to understand why the Ge nanowires melted under these conditions (see Supporting Information). When there was good contact between the 'free' end of the nanowire and the metal electrode, no significant temperature change was observed. However, if the active contact area was thermally isolated, e.g. possibly through a poor contact between the nanowire and the electrode, the temperature rose rapidly, reaching the melting point for bulk Ge in approximately 10^{-7} s. This rapid increase in temperature due to poor contact between the nanowire and the metal electrode is a possible explanation as to why the nanowires melt. However, further work is required to understand this melting phenomenon in more detail.

We did not observe a good match between the calculated elastic forces of the nanowires and the adhesion forces in contact for nanowires at high current densities (Table 1). For nanowires with radii of 60 and 50 nm the values of the calculated elastic forces, 140 and 177 nN, respectively, were lower in comparison to the calculated adhesion forces, i.e. 383 and 339 nN, respectively, which contradicts the fact that jump-off the contact was observed in the experiments. One possibility is that the real contact is modified during the melting process although this needs further investigation. In conclusion, the data presented in this paper demonstrate the potential of using Ge nanowires in mechanically stable two-terminal ON/OFF NEM devices. We have also shown the significant role that the native oxide plays in determining the operation of Ge-based NEM devices and how the oxide can be utilized as a coating to decrease the current density in a device. Such an in-depth study of a two-terminal NEM device based on semiconductor nanowires has not previously been reported.

As has been shown previously,[43,44] for nanocontacts the adhesion forces and the contact area can be described using Maugis theory.[45] Analytical formulas developed by Carpick et al.[46] were used for adhesion force calculations (detailed force calculations can be found in ref 43). The elastic force of a cylindrical nanowire (F) is proportional to the spring constant (k) and the deflection of the nanowire end from the equilibrium position x: $F = -kx$. The spring constant of the beam depends on the beam length L: $k = 12\ EI/L^3$, where E is the Young's modulus, I is the cross sectional moment of inertia.[47] The moment of inertia for a cylindrical nanowire can be calculated as $I = \pi r^4/4$, where r is the radius of the nanowire (detailed forces calculations can also be found in Supporting Information[48−52]).

Acknowledgment. We acknowledge financial support from the ERAF, the Ministry of Education and Science of Latvia, and the Centre for Research on Adaptive Nanostructures and Nanodevices (CRANN) (Project PR21). This research was also enabled by the Higher Education Authority Program for Research in Third Level Institutions (2007−2011) via the INSPIRE programme. We also acknowledge the ESTEEM programme (Contract No. 026019) for access to the high-resolution microscopy facilities at Oxford University.

Supporting Information Available: This material is available free of charge via the Internet at http://pubs.acs.org.

References

(1) Ekinci, K. L.; Roukes, M. L. *Rev. Sci. Instrum.* **2005**, *76*, 061101.
(2) He, R.; Feng, X. L.; Roukes, M. L.; Yang, P. *Nano Lett.* **2008**, *8*, 1756.
(3) Verbridge, S. S.; Craighead, H. G.; Parpia, J. M. *Appl. Phys. Lett.* **2008**, *92*, 013112.
(4) Huang, M. H.; Zorman, C. A.; Mehregany, M.; Roukes, M. L. *Nature (London)* **2003**, *421*, 496.
(5) Sazonova, V.; Yaish, Y.; Üstünel, H.; Roundy, D.; Arias, T. A.; McEuen, P. L. *Nature (London)* **2004**, *431*, 284.
(6) Husain, A.; Hone, J.; Ch. Postma, H. W.; Huang, X. M. H.; Drake, T.; Barbic, M.; Scherer, A.; Roukes, M. L. *Appl. Phys. Lett.* **2003**, *83*, 1240.
(7) Li, M.; Mayer, T. S.; Sioss, J. A.; Keating, C. D.; Bhiladvala, R. B. *Nano Lett.* **2007**, *7*, 3281.

(8) Feng, X. L.; He, R.; Yang, P.; Roukes, M. L. *Nano Lett.* **2007**, *7*, 1953.
(9) Kim, P.; Lieber, C. M. *Science* **1999**, *126*, 2148.
(10) Akita, S.; Nakayama, Y.; Mizooka, S.; Takano, Y.; Okawa, T.; Miyatake, Y.; Yamanaka, S.; Tsuji, S. M.; Nosaka, T. *Appl. Phys. Lett.* **2001**, *79*, 1691.
(11) Lee, S.; Lee, D.; Morjan, R.; Jhang, S.; Sveningsson, M.; Nerushev, O.; Park, Y.; Campbell, E. *Nano Lett.* **2004**, *4*, 2027.
(12) Hwang, H. J.; Kang, J. W. *Physica E* **2005**, *27*, 163.
(13) Ziegler, K. J.; Lyons, D. M.; Holmes, J. D.; Erts, D.; Polyakov, B.; Olin, H.; Olsson, E.; Svensson, K. *Appl. Phys. Lett.* **2004**, *84*, 4074.
(14) Viasnoff, V.; Meller, A.; Isambert, H. *Nano Lett.* **2006**, *6*, 101.
(15) Chen, Z.; Tong, L.; Wu, Z.; Liu, Z. *Appl. Phys. Lett.* **2008**, *92*, 103116.
(16) Jang, J. E.; Cha, S. N.; Choi, Y. J.; Kang, D. J.; Butle, T. P.; Hasko, D. G.; Jung, J. E.; Kim, J. M.; Amaratunga, G. A. J. *Nat. Nanotechnol.* **2008**, *3*, 26.
(17) Jang, W. W.; Lee, J. O.; Joon, J. B.; Kim, M. S.; Lee, J. M.; Kim, S. M.; Cho, K. H.; Kim, D. W.; Park, D.; Lee, W. S. *Appl. Phys. Lett.* **2008**, *92*, 103110.
(18) Ke, C.; Espinosa, H. D. *Small* **2006**, *2*, 1484.
(19) Jang, J. E.; Cha, S. N.; Choi, Y.; Gehan, A. J.; Amaratunga, A. J.; Kang, D. J.; Hasko, H. G.; Jung, J. E.; Kim, J. M. *Appl. Phys. Lett.* **2005**, *87*, 163114.
(20) Rueckes, T.; Kim, K.; Joslevich, E.; Tseng, G. Y.; Cheung, C.-L.; Lieber, C. M. *Science* **2000**, *289*, 94.
(21) Ilic, B.; H. Craighead, G.; Krylov, S.; Senaratne, W.; Ober, C.; Neuzil, P. *J. Appl. Phys.* **2004**, *95*, 3694.
(22) Ekinci, K. L.; Huang, X. M. H.; Roukes, M. L. *Appl. Phys. Lett.* **2004**, *84*, 4469.
(23) Ekinci, K. L.; Yang, Y. T.; Roukes, M. L. *J. Appl. Phys.* **2004**, *95*, 2682.
(24) Yang, Y. T.; Callegari, C.; Feng, X. L.; Ekinci, K. L.; Roukes, M. L. *Nano Lett.* **2006**, *6*, 583.
(25) Ilic, B.; Yang, Y.; Craighead, H. G. *Appl. Phys. Lett.* **2004**, *85*, 2604.
(26) Lee, C.; Radhakrishnan, R.; Chen, C. C.; Li, J.; Thillaigovindan, J.; Balasubramanian, N. *J. Lightwave Technol.* **2008**, *26*, 839.
(27) Roukes, M. L. *Phys. World* **2001**, *14*, 25.
(28) Cho, A. *Science* **2003**, *299*, 36.
(29) Armour, A. D.; Blencowe, M. P.; Schwab, K. C. *Phys. Rev. Lett.* **2002**, *88*, 148301.
(30) Melosh, N. A.; Boukai, A.; Diana, F.; Gerardot, B.; Badolato, A.; Petroff, P. M.; Heath, J. R. *Science* **2003**, *300*, 112.
(31) Kinaret, J.; Nord, T.; Viefers, S. *Appl. Phys. Lett.* **2003**, *82*, 1287.
(32) Li, X. Q.; Koo, S. M.; Richter, C. A.; Edelstein, M. D.; Bonevich, J. E.; Kopanski, J. J.; Suehle, J. S.; Vogel, E. M. *IEEE Trans. Nanotechnol.* **2007**, *6*, 256.
(33) Ryan, K. M.; Erts, D.; Olin, H.; Morris, M. A.; Holmes, J. D. *J. Am. Chem. Soc.* **2003**, *125*, 6284.
(34) Dequesnes, M.; Rotkin, S. V.; Aluru, N. R. *Nanotechnology* **2002**, *13*, 120.
(35) Bulashevich, K. A.; Rotkin, S. V. *JETP Lett. (Engl. Transl.)* **2002**, *75*, 205.
(36) Dujardin, E.; Derycke, V.; Goffman, M. F.; Lefèvre, R.; Bourgoin, J. P. *Appl. Phys. Lett.* **2005**, *87*, 193107.
(37) Holmes, J. D.; Johnston, K. P.; Doty, R. C.; Korgel, B. A. *Science* **2002**, *287*, 1471.
(38) Sze, S. M. *Physics of Semiconductor Devices*; Wiley-Interscience: New York, 1981.
(39) Moore, G. E. *Electronics* **1965**, *38*, 84.
(40) Erts, D.; Olin, H.; Ryen, L.; Olsson, E.; Thölen, A. *Phys. Rev. B: Condens. Mater. Phys.* **2000**, *61*, 12725.
(41) Erts, D.; Lõhmus, A.; Lõhmus, R.; Olin, H. *Appl. Phys. A* **2001**, *72*, S71.
(42) Ngo, L. T.; Almecija, D.; Sader, J. E.; Daly, B.; Petkov, N.; Holmes, J. D.; Erts, D.; Boland, J. J. *Nano Lett.* **2006**, *6*, 2964.
(43) Lantz, M. A.; O'Shea, S. J.; Welland, M. E. *Phys. Rev. B: Condens. Mater. Phys.* **1997**, *56*, 15345.
(44) Erts, D.; Lõhmus, A.; Lõhmus, R.; Olin, H.; Pokropivny, A. V.; Ryen, L.; Svensson, K. *Appl. Surf. Sci.* **2002**, *188*, 460.
(45) Maugis, D. *Contact Adhesion and Rupture of Elastic Solids*; Springer: Berlin, 2000.
(46) Carpick, R. W.; Ogletree, D. F.; Salmeron, M. *J. Colloid Interface Sci.* **1999**, *211*, 395.
(47) Timoshenko, S.; Goodier, J. *Theory of Elasticity*; McGraw-Hill: New York, 1970.
(48) Johnson, K. L.; Kendall, K.; Roberts, A. D. *Proc. R. Soc. London, Ser. A* **1971**, *324*, 301.
(49) Derjaguin, B. V.; Muller, V. M.; Toporov, Y. P. J. *J. Colloid Interface Sci.* **1975**, *53*, 314.
(50) Tabor, D.; Winterton, R. H. S. *Proc. R. Soc. London, Ser. A* **1975**, *312*, 435.
(51) Maugis, D. *J. Colloid Interface Sci.* **1992**, *150*, 243.
(52) Agrait, N.; Rubio, G.; Vieira, S. *Langmuir* **1996**, *12*, 4505.

NL8037807